Human autoimmunity after lymphocyte depletion is caused by homeostatic T-cell proliferation

Joanne L. Jones[a,1], Sara A. J. Thompson[a], Priscilla Loh[b], Jessica L. Davies[a], Orla C. Tuohy[a], Allison J. Curry[a], Laura Azzopardi[a], Grant Hill-Cawthorne[a,c], Michael T. Fahey[b,d], Alastair Compston[a], and Alasdair J. Coles[a]

[a]Department of Clinical Neurosciences, University of Cambridge, Cambridge CB2 0QQ, United Kingdom; [b]Division of Mathematics, Informatics and Statistics, Commonwealth Scientific and Industrial Research Organization, Clayton South, VIC 3169, Australia; [c]Sydney Institute for Emerging Infections and Biosecurity, University of Sydney, Sydney, NSW 2006, Australia; and [d]Biostatistics Unit, Monash University, Melbourne, VIC 3004 Australia

The association between lymphopenia and autoimmunity is recognized, but the underlying mechanisms are poorly understood and have not been studied systematically in humans. People with multiple sclerosis treated with the lymphocyte-depleting monoclonal antibody alemtuzumab offer a unique opportunity to study this phenomenon; one in three people develops clinical autoimmunity, and one in three people develops asymptomatic autoantibodies after treatment. Here, we show that T-cell recovery after alemtuzumab is driven by homeostatic proliferation, leading to the generation of chronically activated (CD28−CD57+), highly proliferative (Ki67+), oligoclonal, memory-like CD4 and CD8 T cells (CCR7−CD45RA− or CCR7−CD45RA+) capable of producing proinflammatory cytokines. Individuals who develop autoimmunity after treatment are no more lymphopenic than their nonautoimmune counterparts, but they show reduced thymopoiesis and generate a more restricted T-cell repertoire. Taken together, these findings demonstrate that homeostatic proliferation drives lymphopenia-associated autoimmunity in humans.

T lymphocytes | reconstitution | immunotherapy

The anti-CD (cluster of differentiation molecule) 52 monoclonal antibody alemtuzumab has proven efficacy in relapsing remitting multiple sclerosis (RRMS) (1–3). Each cycle of alemtuzumab leads to profound panlymphopenia, but relatively infrequent dosing allows reconstitution to occur: B cells recovery rapidly, whereas CD4 and CD8 cells take 35 and 20 mo, respectively, to reach normal values (4). For 5 y after alemtuzumab and maximally, at 2 y, secondary autoimmune conditions may develop: 30% of individuals experience thyroid autoimmunity, and 1% of individuals have idiopathic thrombocytopenic purpura (ITP); there are rare cases of autoimmune hemolytic anemia, autoimmune neutropenia, and Goodpasture syndrome (1–3). One-third of patients develop asymptomatic autoantibodies.

An association between lymphopenia and autoimmunity is recognized; in humans, T lymphopenia is a feature of systemic lupus erythematosus, rheumatoid arthritis, and Crohn and Sjogren syndromes (5), and animal models of autoimmunity often involve the induction of lymphopenia. The mechanism driving autoimmunity in these situations is unclear. In some cases it has been attributed to loss of regulatory cells; however, although treatment of lymphopenic hosts with CD4+CD25+ Tregs can abrogate autoimmunity induced by cotransferred CD25− cells, depletion of Tregs from T-replete animals rarely evokes autoimmunity (6).

Recovery from T lymphopenia may occur by (i) thymopoiesis resulting in clonally diverse naive cells or (ii) homeostatic proliferation (HP) of cells that have escaped depletion. Much of what we know about HP comes from experiments in which T cells are adoptively transferred into irradiated or immune-deficient animals. These studies show that HP is driven by cytokines and in part, by recognition of self-MHC/peptide ligands (7, 8). Because homeostatically proliferating T cells acquire the characteristics of effector memory cells (9–11), it has been proposed that this

process may lead to the breakdown of self-tolerance. However, only two studies (both in mice) have directly shown a role for HP in autoimmunity [promoting diabetes in the nonobese diabetic mouse driven by IL-21 in one study (12) and inducing autoimmune pancreatitis after transfer of T cells expressing hemagglutinin (HA)-specific T cell receptors (TCRs) into sublethally irradiated InsHA transgenic mice (which express HA in the beta cells of the pancreas) in another study (13)].

Although informative, these complex models cannot be assumed to accurately reflect the process that drives human autoimmunity. Therefore, we take advantage of our unique patient population here to characterize T-cell reconstitution and the development of autoimmunity after lymphocyte depletion directly in humans.

Results

Autoimmunity Is Unrelated to Rate of T-Cell Reconstitution. CD4 and CD8 counts from 87 patients were analyzed. All patients received two cycles of alemtuzumab (usually 12 mo apart); additional cycles were triggered by clinical or radiological evidence of multiple sclerosis (MS) disease activity. Data from one patient was excluded because of treatment with rituximab for postalemtuzumab ITP (*SI Appendix*, Table S1). As previously reported, T lymphopenia after alemtuzumab was prolonged, and recovery occurred in two linear phases—a fast phase for 18 mo followed by a slower phase (4). Reconstitution rates were estimated by performing separate linear regressions on these two phases for each patient–treatment combination. Rate of the CD4 fast phase declined with age, and therefore, subsequent analyses were age-adjusted. The fast phase of CD4 and CD8 reconstitution declined with successive treatments (P < 0.001) (Fig. 1A and *SI Appendix*, Tables S2 and S3); the slow phase was unaffected.

Significance

This paper identifies the mechanism by which patients with multiple sclerosis develop secondary autoimmunity after treatment with the lymphocyte-depleting humanized monoclonal antibody alemtuzumab (Campath-1H). In identifying this mechanism, it shows that T-cell homeostatic proliferation can lead to autoimmunity in humans. Alemtuzumab is one of the most effective treatments of multiple sclerosis tested to date; it is currently licensed in the European Union and under consideration by the Food and Drug Administration. Understanding what drives its most significant side effect is of clear clinical importance.
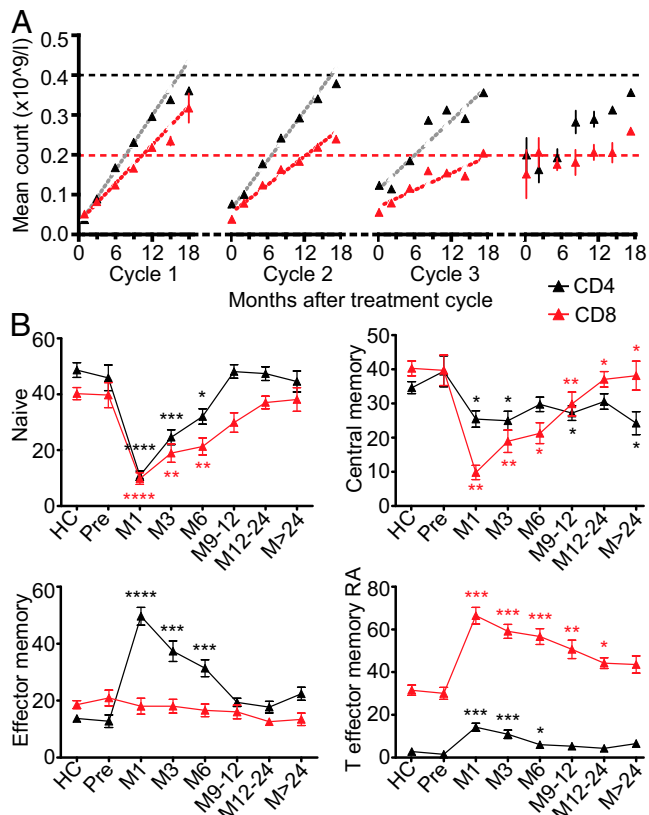
Fig. 1. CD4 and CD8 reconstitution slows with repeated cycles and is dominated by effector memory populations. (*A*) Mean CD4 and CD8 counts ± SEM up to 18 mo after each cycle. Dotted horizontal lines represent the lower limits of normal, and dashed lines represent the fitted models. There were too few data points for the model to be reliably fitted after cycle 4. (*B*) Mean CD4 and CD8 subsets ± SEM from 29 healthy controls (HCs) and 87 RRMS patients pre- and postalemtuzumab. *$P < 0.05$; **$P < 0.01$; ***$P < 0.001$; ****$P < 0.0001$.

Sixty-six percent of these patients (57/87) developed autoimmunity after alemtuzumab; 40 of 87 (46%) patients developed clinical autoimmunity (36 patients, thyroid; 3 patients, ITP; 1 patient, Goodpasture syndrome), and 17 of 87 (20%) patients developed persistent asymptomatic novel autoantibodies (*SI Appendix*, Table S4). CD4 and CD8 cell reconstitution was similar between those patients with and without autoimmunity (*SI Appendix*, Table S5).

Highly Proliferative Effector Memory Populations Dominate After Alemtuzumab. In a cross-section of 86 patients and 22 healthy individuals (*SI Appendix*, Table S6), CD45RA$^+$/CCR7$^+$ phenotypically naive (CD4/8$_{naive}$) cells were reduced for 6 mo, and CD45RA$^+$CCR7$^+$ central memory (CD4/8$_{CM}$) cells were low throughout (Fig. 1*B*). Consistent with HP, reconstitution was dominated by T cells with effector memory phenotypes, especially in the CD8 pool, where CD45RA$^+$CCR7$^-$ T-effector memory RA (CD8$_{TEMRA}$) cells accounted for 40–70% of circulating CD8 cells for at least 24 mo (Fig. 1*B*). Within the CD4 pool, CD45RA$^-$CCR7$^-$ effector memory (CD4$_{EM}$) cells were expanded for 6 mo after treatment, and CD4$^+$CD45RA$^+$CCR7$^-$ (CD4$_{TEMRA}$) cells were substantially increased for 6–9 mo; normally rare, for 3 mo, they represented >10% of circulating CD4 cells (Fig. 1*B*). CD4 and CD8 Ki67 expression was increased for up to 2 y after alemtuzumab, suggesting sustained peripheral proliferation (Fig. 2*A*) except in CD8$_{TEMRA}$ cells, which is in line with their proposed terminally differentiated state and loss of proliferative capacity (*SI Appendix*, Fig. S1).

Likewise, all cells except CD8$_{TEMRA}$ showed markers of increased activation (HLA-DR) and susceptibility to Fas-mediated apoptosis (CD95) (Fig. 2*A* and *SI Appendix*, Fig. S1). Reconstituted CD4 and CD8 cells showed evidence of chronic activation and repeated cell division: reduced expression of CD127 (IL-7Rα) and CD28 (particularly CD8 cells) and increased CD8 CD122 (IL-2R/15Rβ) expression (Fig. 2*A* and *SI Appendix*, Fig. S1). CD57, indicating replicative senescence (14), was up-regulated for 3 mo on CD4 cells and 9 mo on CD8 cells, especially CD8$_{TEMRA}$ cells (Fig. 2*A* and *SI Appendix*, Fig. S1). CD4 expression of the inhibitory receptors [programmed death-1 (PD-1) and lymphocyte activation gene-3 (LAG-3)] was increased 6–9 mo after alemtuzumab (Fig. 2*A*).

Expanded CD8$_{TEMRA}$ Population Has Cytotoxic Potential. CD28$^-$CD57$^+$ CD8$^+$$_{TEMRA}$ cells have been reported with chronic viral infection and aging, and they are variably described as senescent, cytotoxic, or immunosuppressive. After alemtuzumab, they did not acquire a regulatory phenotype; FoxP3 and PD-1 expression did not increase, nor did they suppress CD4$^+$CD25$^-$ effector proliferation; rather, they contained perforin and granzyme B (*SI Appendix*, Figs. S1 and S2) and produced significant IFNγ and TNFα on stimulation, showing effector capacity (Fig. 2*B*). IL-2 production was low compared with CD8 non-TEMRA, and it did not increase poststimulation, which may reflect early exhaustion (15).

Postalemtuzumab Homeostatic Proliferation Generates Activated Tregs. As previously reported (16, 17), cells with a regulatory phenotype CD4$^+$CD25^{hi}CD127^{lo} were increased relative to

Fig. 2. T cells after alemtuzumab show evidence of chronic activation and have cytotoxic potential. (*A*) Mean percentage of the parent population expressing a given maker ± SEM: a cross-sectional analysis of 86 patients pre- and post-alemtuzumab vs. 29 HCs. HLADR, human leukocyte antigen-DR. (*B*) Mean percentage of cytokine positive cells ± SEM from 11 patients postalemtuzumab. ns, not significant. *$P < 0.05$; **$P < 0.01$; ***$P < 0.001$; ****$P < 0.0001$.
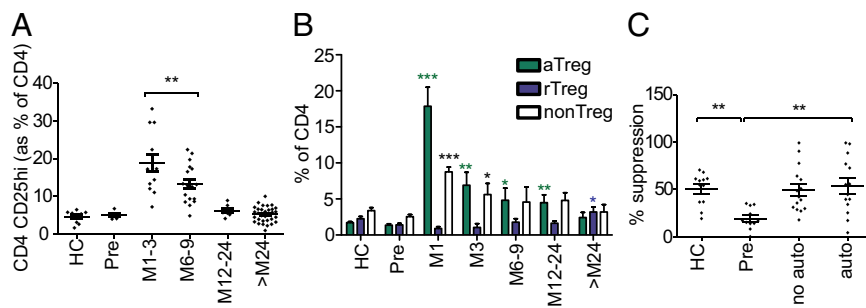
Fig. 3. Mature aTregs are expanded after alemtuzumab, and long-term functional regulation is restored. (*A*) Percentage of CD4 cells with a CD4$^+$CD25^{hi} Treg phenotype. (*B*) Percentage of CD4 with an aTreg (CD45RA$^-$FoxP3hi) vs. rTreg (CD45RA$^+$FoxP3lo) vs. non-Treg (CD45RA$^-$FoxP3lo) phenotype. (*C*) Suppressive capacity of CD4$^+$CD25hi Tregs from 29 patients 3–4 y postalemtuzumab compared with 12 healthy controls. All graphs show mean ± SEM. *P < 0.05; **P < 0.01; ***P < 0.001.

other CD4 subsets for 9 mo after alemtuzumab (Fig. 3*A*). We now show that these cells have a mature/activated phenotype (aTreg) being CD45RA$^-$FoxP3^{hi} and CD31$^-$, suggesting that they are not of recent thymic origin (Fig. 3*B* and *SI Appendix,* Fig. S3). Indeed, recent thymic CD31$^+$ naive/resting Tregs (rTregs; CD45RA$^+$FoxP3^{lo}) were reduced after treatment (Fig. 3*B* and *SI Appendix,* Fig. S3).

The expanded aTreg population expressed high Helios (*SI Appendix,* Fig. S3); although originally reported to distinguish natural Tregs from induced Tregs (18), Helios is now considered a marker of activation regardless of cell subset (19). In keeping with this observation, rTreg Helios was low. The expanded aTreg population also expressed high CD39, whereas rTreg CD39 was low (*SI Appendix,* Fig. S3), confirming that, in humans, CD39 expression is restricted to memory Tregs (20). CD39$^+$ Tregs have been shown to be deficient in MS patients (20). Because of low recoverable cell numbers, we have been unable to confirm the suppressive function of this expanded putative Treg population early after alemtuzumab. However, we have shown that CD4$^+$CD25^{hi} cells from patients 3–4 y after treatment are normally suppressive, equivalent to healthy controls and greater than untreated patients (Fig. 3*C*); no difference was seen between patients with and without autoimmunity.

Thymopoiesis Is Reduced After Alemtuzumab. As a proportion of CD4, recent thymic emigrants (CD31$^+$CD4$_{naive}$) (21) fell for 3 mo posttreatment and then, returned to baseline; absolute recent thymic emigrants remained low throughout (Fig. 4*A*). The Sj/β T-cell receptor excision circle (TREC) ratio, which reflects intrathymic proliferation and is uncompromised by peripheral cell division (22), showed a trend to reduced thymic function in RRMS patients compared with healthy controls as previously reported (23). For 6 mo after alemtuzumab, the Sj/βTREC ratio was further reduced, reflecting diminished thymic function (Fig. 4*B*).

T-Cell Clonality Is Reduced After Alemtuzumab, Particularly Within the CD8 Pool. If T-cell reconstitution is driven by HP, one would expect the resultant pool to be oligoclonal; to assess this prediction, we performed TCRβ CDR3 spectratyping in 22 patients with RRMS pre- and postalemtuzumab. Spectratyping showed increased unde-

tectable V-β (BV) families and reduced mean complexity (24) of the remaining families (Fig. 5*A*), confirming an oligoclonal repertoire. CD8 cells from patients <12 mo after alemtuzumab were more restricted than their CD4 counterparts, but CD8 cells were not more restricted beyond 2 y (Fig. 5*B*). Given the difficulties of detecting low-frequency clones by spectratyping, we sequenced TCRβ CDR3 of CD4 and CD8 cells from one patient at 3 mo and another patient at 12 mo postalemtuzumab: CD4 and CD8 variable(V)-joining(J) diversity was more restricted at month 3 than month 12 postalemtuzumab and most marked in the CD8 subset (Fig. 5*C* and *SI Appendix,* Fig. S5).

T-Cell Homeostatic Proliferation Drives Autoimmunity After Alemtuzumab. Next, we asked if HP drives autoimmunity after alemtuzumab. To answer this question we determined the relative contribution of HP vs. thymopoiesis to T-cell recovery by measuring TCR clonality (spectratyping and sequencing) and intrathymic proliferation (Sj/βTREC) in patients with and without autoimmunity. Because these assays can be performed on stored cells, we were able to study reconstitution before the onset of autoimmunity in a cohort whose long-term autoimmune status was confirmed. Those patients who developed autoimmunity after alemtuzumab showed greater clonal restriction by both sequencing (increased high-frequency clones) (Fig. 6*A*) and spectratyping (more undetectable BV families and reduced complexity of the remaining families) (Fig. 6*B*) compared with the no autoimmune cohort. No difference was seen between those patients with clinical autoimmunity vs. autoantibodies alone; however, the autoantibody cohort was small (Fig. 6). Next, we followed reconstitution by serial TCR sequencing in two patients. Both patients had received two cycles of alemtuzumab and been followed for >7 y: patient A (male; 32 y) had not developed autoimmunity, whereas patient B (female; 25 y) developed Graves disease 15 mo after cycle 2. By month 6, patient A's TCR diversity had recovered, and at 12 mo, it was more diverse than pretreatment, whereas patient B's T-cell pool remained oligoclonal at 12 mo. In both patients, it was the baseline high-frequency clones that expanded posttreatment (*SI Appendix,* Fig. S6). Finally, thymopoiesis was reduced at 12 mo posttreatment in the cohort that subsequently developed autoimmunity (n = 16; 14
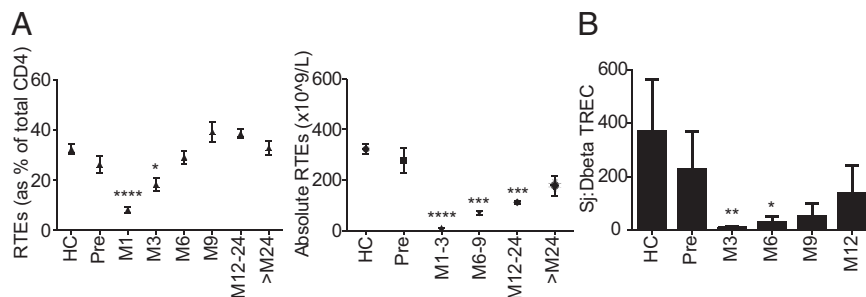

Fig. 4. Thymic function is reduced after alemtuzumab. (*A*) Percentage and absolute number of CD4 cells with recent thymic emigrants (RTEs) phenotype (CD4$^+$CD45RA$^+$CCR7$^+$CD31$^+$). (*B*) Sj/βTREC ratio in a cross-sectional analysis of 12 healthy controls vs. 12 RRMS patients pre- and postalemtuzumab. All graphs show mean ± SEM. *P < 0.05; **P < 0.01; ***P < 0.001; ****P < 0.0001.
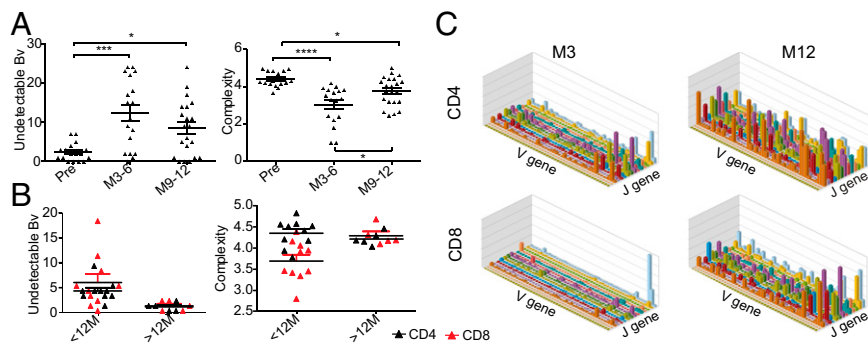
Fig. 5. T-cell clonality is reduced after alemtuzumab. (A) CDR3 spectratyping of 22 RRMS patients pre- and postalemtuzumab; mean numbers of undetectable BV families and mean complexity scores for detectable families are shown ± SEM. (B) CD4 and CD8 cells from 10 patients <12 mo of treatment and 5 patients >2 y postalemtuzumab. (C) TCR sequencing of CD4 and CD8 cells from one patient 3 mo after alemtuzumab and a second patient 12 mo posttreatment. V-J histograms are shown. *P < 0.05; **P < 0.01; ***P < 0.001; ****P < 0.0001.

thyroid and 2 autoantibodies only) compared with those patients without autoimmunity (n = 10) (Fig. 6C).

Combined with the observation that the autoimmune cohort was no more lymphopenic than the nonautoimmune group, these findings support the hypothesis that HP leads to the autoimmunity after alemtuzumab.

Discussion

Our unique patient population has provided us a rare chance to study T-cell reconstitution and autoimmunity in humans. We have shown that early T-cell recovery is largely by homeostatic expansion of cells that have escaped depletion, a conclusion that is supported by the predominance of highly proliferative memory-like cells, the oligoclonal nature of the resulting repertoire, and lack of a thymic response during reconstitution. We have previously reported that the postalemtuzumab T-cell pool is enriched for autoreactive cells, suggesting that this process is, in part, driven by TCR self-antigen engagement (25). By showing that exaggerated HP increases and greater thymic response decreases the risk of autoimmunity after alemtuzumab, we show that HP promotes lymphopenia-associated autoimmunity in humans.

We initially assessed thymic function by assaying $CD31^+$ recent thymic emigrants (21). However, this method is inexact: $CD4_{naive}$ cells can proliferate without loss of CD31 (26), and most $CD31^+CD4_{naive}$ cells are derived from peripheral proliferation (27). Furthermore, $CD31^+$ may persist on TCR activa-

tion (28), and IL-7, known to be increased postalemtuzumab (16), induces proliferation of $CD31^+CD4_{naive}$ cells without loss of CD31 (29). Therefore, we adopted a second strategy to assess thymopoiesis—the Sj/βTREC ratio. TRECs are byproducts of TCR gene rearrangement. The SjTREC/cell is a widely used measure of thymopoiesis; however, it can be difficult to interpret in the setting of lymphopenia, because TRECs do not replicate and thus, are diluted out by peripheral division. The Sj/βTREC ratio circumvents this problem, because it is generated by proliferation that occurs between TCRB rearrangement and excision of the TCRd locus; as such, it is a measure of thymic activity (22, 30). It is unaffected by extrathymic proliferation, because both TRECs are similarly diluted on cell division. Unexpectedly, both measures showed reduced thymic function after alemtuzumab, perhaps because of intrathymic T-cell depletion (although intrathymic T-cell depletion was minimal in the huCD52 transgenic mouse) (31) or the thymosuppressive effects of IL-6 and other cytokines released during alemtuzumab-induced cytolysis (32).

Restricted TCR clonality was shown by spectratyping and sequencing. The latter showed that the most highly expressed clones pretreatment were the ones that expanded afterward. Over time, clonality increased, showing that thymopoiesis does contribute to recovery in the long term if not acutely. HP was most marked for CD8 cells, which was shown by more rapid recovery, marked phenotypic skewing to TEMRAs, and reduced clonality compared with CD4. This finding may reflect reduced

Fig. 6. T-cell homeostatic proliferation drives autoimmunity after alemtuzumab. (A) Clonal frequency in 5 patients without autoimmunity vs. 13 patients with autoimmunity (10 thyroid and 2 autoantibodies) at 6 mo and clonal frequency in 7 nonautoimmune vs. 11 autoimmune patients (9 thyroid and 2 autoantibodies) at 12 mo postalemtuzumab. (B) CDR3 spectratyping of nine autoimmune patients (six thyroid and three autoantibodies) vs. nine nonautoimmune patients 12 mo postalemtuzumab. Mean undetectable BV subfamilies and mean complexity scores for detectable subfamilies are shown ± SEM. (C) Mean absolute and mean Sj/βTREC ratios relative to baseline ± SEM in 10 patients without autoimmunity vs. 16 patients with autoimmunity (14 thyroid and 2 autoantibodies)12 mo after alemtuzumab. *P < 0.05; **P < 0.01.

responsiveness of CD4 cells to HP cues, such as IL-7 (9, 33). Here, we show that CD4 expansion may also be limited by upregulation of the inhibitory receptors PD-1 and LAG-3 and prolonged CD95 (Fas) expression (34, 35).

CD28$^-$CD57$^+$CD8$_{TEMRA}$ dominated the CD8 pool for >9 mo postalemtuzumab. These cells occur in chronic viral infections and aging, and they have variably been described as exhausted, senescent, cytotoxic, or immunosuppressive (36). They are also associated with autoimmunity, including Graves disease (37). CD8$_{TEMRA}$ cells after alemtuzumab were not regulatory; they expressed low FoxP3 and PD-1 (38), and they failed to suppress CD4 effectors. Instead, they expressed perforin and Granzyme B and produced IFNg and TNFa after stimulation, showing potential pathogenicity.

As we and others have reported, cells with a regulatory phenotype are increased relative to other T cells after alemtuzumab (16, 17). Here, we show that they have a mature/activated phenotype (CD45RA$^-$FoxP3^{hi}CD31$^-$Helios$^+$), suggesting that they arise from HP. After alemtuzumab, Tregs express high CD39, which is required for effective immunoregulation (39); CD39$^+$Tregs are known to be defective in MS (20). CD4 Tregs at 3–4 y after alemtuzumab have greater capacity for suppression than before treatment, which is equivalent to healthy controls; low recoverable cell numbers prevented assessment at earlier time points. However, even if early Tregs are functional, they are not sufficient to prevent autoimmunity in many patients, perhaps because of the enhanced ability of HP-driven T cells to resist regulation (40).

Autoimmunity after alemtuzumab develops when HP dominates reconstitution over thymopoiesis. Why one patient should mount an exaggerated HP response and/or a reduced thymic response is not fully understood, but it is likely to reflect a complex interplay of genetic background, exposure to exogenous antigens, thymic reserve, and release of homeostatic cytokines. We have previously reported raised serum IL-21, which is related to the IL-21 genotype, in patients who develop autoimmunity after alemtuzumab (25). We speculate that high rates of autoimmunity in our patients, compared with non-MS patients treated with alemtuzumab, reflect their proautoimmune background and known reduced thymic function. Predilection for the thyroid may arise genetically; families with members affected by MS have higher rates of thyroid disease (41, 42). Consistent with this hypothesis is the observation that pretreatment anti-TPO antibodies predispose patients to thyroid disease after alemtuzumab. Although postalemtuzumab autoimmunity is associated with autoantibodies, the lack of secondary autoimmunity after B-cell depletion therapy of MS (43) suggests that maladaptive reconstitution of T cells (rather than B cells) is at fault. Reassuringly, alemtuzumab is equally efficacious in suppressing MS disease activity in patients with and without secondary autoimmunity (44).

We have shown that HP of residual T cells and failure of thymic reconstitution drive lymphopenia-associated autoimmunity in humans. In addition to shedding light on the most important side effect of a drug soon to enter clinical practice, our findings offer a note of caution for the increasing use of depleting monoclonals in transplantation, and they may explain the disappointing results of using alemtuzumab without conventional immunosuppression (45, 46). Another inference is that autoimmunity after alemtuzumab may be reduced by disrupting HP. We are testing this approach by giving keratinocyte growth factor combined with alemtuzumab to patients with RRMS to drive T-cell recovery through the thymus rather than by expansion of residual cells (ClinicalTrials.gov; NCT01712945).

Materials and Methods

Subjects and Samples. All patients had RRMS, were treated in Cambridge, United Kingdom, and participated in CAMMS-224 [Research Ethics Committee (REC):REC 03/078], CAMMS-223 (phase 2), or Comparison of Alemtuzumab and Rebif Efficacy in Multiple Sclerosis-1 (CAREMS-1) or Comparison

of Alemtuzumab and Rebif Efficacy in Multiple Sclerosis-2 (CAREMS-2) (phase 3). Alemtuzumab was given for 5 d at baseline and 3 d at month 12; furthermore, 3-d cycles were triggered by clinical or radiological evidence of disease activity. All patients consented to long-term follow-up (CAMSAFE REC 11/33/0007). Secondary autoimmunity was defined as (i) symptomatic autoimmune disease (excluding MS) or (ii) new autoantibodies detected above the normal range on two or more occasions ≥3 mo apart (25). CD4/CD8 counts and serum autoantibodies were measured every 3 mo for up to 3 y after each cycle of alemtuzumab and every 6–12 mo thereafter. Peripheral blood mononuclear cells (PBMCs) were prepared as previously reported (25). Patient details for each assay are given in below.

Immunophenotyping. PBMCs from 86 patients with RRMS and 29 healthy controls (SI Appendix, Table S6) were phenotyped using antibodies against CD8-V500, CD4-APC, CD4-V500, CD45RA-PECy5, CD45RA-PECy7, CCR7-FITC, CCR7-PE, CD127-V450, CD279-PECy7, CD57-PE, CD28-PECy7, CD122-PE, CD31-V450, CD31-FITC, CD95-V450, HLADR-PECy7, CD25-PE, CD39-APC, Perforin PE, Granzyme-B V450, Ki67 PE, FoxP3 PE, and Helios APC (BD Biosciences) as well as LAG3-PE (R&D Systems). Intracellular staining was performed on fixed permeablized cells using Cytofix/Cytoperm (BD Bioscience) for cytoplasmic antigens or FoxP3 Transcription Factor Buffer Set (eBioscience) for nuclear antigens. Analysis was with Flow Jo (Tree Star Inc.)

Intracellular Cytokine Production. Freshly isolated PBMCs from 11 patients (8 females; mean = 9.7 mo after alemtuzumab) were stained with CD8-V500, CD45RA-PECy5, and CCR7-FITC, and they were FACS-sorted into three populations: CD8$^+$CD45RA$^+$CCR7$^-$$_{TEMRA}$, all other CD8$^+$ cells, and all other CD8$^-$ cells; 10^6 cells/mL sorted cells were cultured in RPMI 1% (vol/vol) penicillin/streptomycin and 10% (vol/vol) FCS (S5394; Sigma-Aldrich) with or without phorbol myristate acetate (50 ng/mL) and Ionomycin (1 μg/mL) plus monensin (2 μM GolgiStop). Six hours later, cells were harvested and stained with antibodies against IFNg-APC, TNFa-V450, and IL2-PE (BD Bioscience).

In Vitro Suppression Assay. Suppression assays were performed on 11 patients prealemtuzumab, 29 patients 3–4 y postalemtuzumab (14 patients with autoimmunity), and 12 healthy controls. CD4$^+$CD25^{hi} cells were isolated using magnetic beads (Regulatory T-Cell Isolation Kit; Miltenyi Biotec). Briefly, CD4 cells were negatively selected followed by two rounds of CD25$^+$ positive selection to maximize purity; 5 × 10^4 CD4$^+$CD25$^-$ responder T cells (Tresps) were cultured in RPMI/10% human AB serum with or without CD3/CD28 beads (1:1 bead:cell) at Tresp:CD4$^+$CD25^{hi} Tregs ratios of 1:1, 2:1, 4:1, and 8:1. Proliferation was measured after 72 h by an MTT [3-(4,5-dimethylthiazol-2-yl)-2,5-diphenyl tetrazolium bromide] assay, with absorbance reads at 570 nm expressed as percentage suppression compared with proliferation of stimulated Tresps.

DNA and RNA Extraction. Genomic DNA and total RNA were isolated from frozen PBMCs or bead-separated CD4 and CD8 cells using the Qiagen Allprep method. RNA was then reverse transcribed into cDNA (AffinityScript Multiple Temperature cDNA Synthesis Kit; Stratagene).

Intrathymic Proliferation—Measurement of Sj/βTRECs. First, a multiplex PCR was carried out using outer primers for the Sj/βTREC (δREC-ψJα) or each of the six Dβ1-Jβ1 TRECs (Dβ1-Jβ1.6) and the CD3γ chain (SI Appendix, Table S7); 10 μl sample or standard plasmid (about 10^8 copies/μl) containing one copy each of the CD3 gene and either the Sj/βTREC (plasmid sjCD3) or the Dβ1 fragment (plasmid Dβ1) were added to 90 μl PCR mix (ROX Kit 204743; Qiagen). PCR conditions were 15 min denaturation at 95 °C, 22 cycles at 94 °C, 30 s at 60 °C, and 2 min at 72 °C. Samples and standards were then serially diluted 1:10. The second PCR used inner primers (SI Appendix, Table S7) with Lightcycler conditions: 15 min denaturation, 40 cycles at 95 °C, 15 s at 60 °C, reading, and 10 s at 72 °C followed by melting at 95 °C for 1 s, 40 °C for 30 s, and 95 °C for 1 s (ramp 0.2 °C—continuous reading). TRECs were quantified in triplicate. Sj/βTREC ratio was mean (SjTREC/0.5 × CD3)/mean (Dβ1TRECs/0.5 × CD3).

CDR3 Spectratyping. Frozen samples from 22 patients followed longitudinally and 15 patients followed cross-sectionally were spectratyped using primers that amplified sequences of all functional TCR BV families (SI Appendix, Table S9). Briefly, 25 individual PCR reactions were performed using 25 BV-specific forward primers and a BC-specific reverse primer labeled with FAM or HEX. PCR conditions were denaturing at 94 °C for 3 min, 35 cycles of 94 °C for 30 s, 58 °C for 30 s, and 72 °C for 50 s, and then, 72 °C for 2 min. PCR products were detected on an Applied Biosystems 3730xl Sequencer, and data were analyzed using Peak Scanner (Applied Biosystems). Numbers of undetectable

BV families were counted, and mean complexity scores derived from the sum of all peak heights/sum of major peaks × number of major peaks (those peaks with spectratype histogram amplitude ≥ 10% sum of all peak heights) (47).

TCR Sequencing. Immunoseq (Adaptive) performed TCRβ sequencing. After correction for PCR bias, the relative abundance of each CDR3 sequence was calculated (48). Adaptive custom software allowed the reconstitution of individual clones to be tracked.

Statistical Analysis. To study reconstitution, 1,604 CD4 and CD8 counts from 86 and 87 patients, respectively, distributed over four treatment cycles were analyzed (*SI Appendix*, Table S1). Using a piecewise linear regression model fitted separately to each treatment occasion, two summary statistics were generated for each patient-cycle: (*i*) rate of change < 18 mo and (*ii*) rate of change > 18 mo. Random effects analyses accounted for the fact that, for each individual, the computed statistics were not independent over treatment occasions.

Because age at treatment was found to affect reconstitution, results were age-adjusted. To test whether rate of change in the first 18 mo predicted auto-immunity, a logistic regression analysis was performed. Rate of change was categorized into tertiles for use as a predictor. Strength of association was measured by odds ratio and expressed compared with the rate of change in the first tertile. All other data were analyzed using GraphPad Prism 5. To compare two groups, after assessment for normality (D'Agostino and Pearson omnibus tests), a two-tailed *t* or Mann–Whitney test was performed. To compare three or more groups, a one-way ANOVA or Kruskal–Wallis test was performed followed by Dunnett or Dunn correction for multiple comparisons. Corrected *P* values are stated throughout the text.

1. Cohen JA, et al. (2012) Alemtuzumab versus interferon beta 1a as first-line treatment for patients with relapsing-remitting multiple sclerosis: A randomised controlled phase 3 trial. *Lancet* 380(9856):1819–1828.
2. Coles AJ, et al. (2008) Alemtuzumab vs. interferon beta-1a in early multiple sclerosis. *N Engl J Med* 359(17):1786–1801.
3. Coles AJ, et al. (2012) Alemtuzumab for patients with relapsing multiple sclerosis after disease-modifying therapy: A randomised controlled phase 3 trial. *Lancet* 380(9856):1829–1839.
4. Hill-Cawthorne GA, et al. (2012) Long term lymphocyte reconstitution after alemtuzumab treatment of multiple sclerosis. *J Neurol Neurosurg Psychiatry* 83(3):298–304.
5. Khoruts A, Fraser JM (2005) A causal link between lymphopenia and autoimmunity. *Immunol Lett* 98(1):23–31.
6. McHugh RS, Shevach EM (2002) Cutting edge: Depletion of CD4+CD25+ regulatory T cells is necessary, but not sufficient, for induction of organ-specific autoimmune disease. *J Immunol* 168(12):5979–5983.
7. Kassiotis G, Zamoyska R, Stockinger B (2003) Involvement of avidity for major histocompatibility complex in homeostasis of naive and memory T cells. *J Exp Med* 197(8):1007–1016.
8. Kieper WC, Burghardt JT, Surh CD (2004) A role for TCR affinity in regulating naive T cell homeostasis. *J Immunol* 172(1):40–44.
9. Cho JH, Kim HO, Surh CD, Sprent J (2010) T cell receptor-dependent regulation of lipid rafts controls naive CD8+ T cell homeostasis. *Immunity* 32(2):214–226.
10. Goldrath AW, Bogatzki LY, Bevan MJ (2000) Naive T cells transiently acquire a memory-like phenotype during homeostasis-driven proliferation. *J Exp Med* 192(4):557–564.
11. Murali-Krishna K, Ahmed R (2000) Cutting edge: Naive T cells masquerading as memory cells. *J Immunol* 165(4):1733–1737.
12. King C, Ilic A, Koelsch K, Sarvetnick N (2004) Homeostatic expansion of T cells during immune insufficiency generates autoimmunity. *Cell* 117(2):265–277.
13. Le Saout C, Mennechet S, Taylor N, Hernandez J (2008) Memory-like CD8+ and CD4+ T cells cooperate to break peripheral tolerance under lymphopenic conditions. *Proc Natl Acad Sci USA* 105(49):19414–19419.
14. Brenchley JM, et al. (2003) Expression of CD57 defines replicative senescence and antigen-induced apoptotic death of CD8+ T cells. *Blood* 101(7):2711–2720.
15. Wherry EJ (2011) T cell exhaustion. *Nat Immunol* 12(6):492–499.
16. Cox AL, et al. (2005) Lymphocyte homeostasis following therapeutic lymphocyte depletion in multiple sclerosis. *Eur J Immunol* 35(11):3332–3342.
17. Bloom DD, et al. (2008) CD4+ CD25+ FOXP3+ regulatory T cells increase de novo in kidney transplant patients after immunodepletion with Campath-1H. *Am J Transplant* 8(4):793–802.
18. Thornton AM, et al. (2010) Expression of Helios, an Ikaros transcription factor family member, differentiates thymic-derived from peripherally induced Foxp3+ T regulatory cells. *J Immunol* 184(7):3433–3441.
19. Akimova T, Beier UH, Wang L, Levine MH, Hancock WW (2011) Helios expression is a marker of T cell activation and proliferation. *PLoS One* 6(8):e24226.
20. Borsellino G, et al. (2007) Expression of ectonucleotidase CD39 by Foxp3+ Treg cells: Hydrolysis of extracellular ATP and immune suppression. *Blood* 110(4):1225–1232.
21. Kimmig S, et al. (2002) Two subsets of naive T helper cells with distinct T cell receptor excision circle content in human adult peripheral blood. *J Exp Med* 195(6):789–794.
22. Dulude G, et al. (2008) The magnitude of thymic output is genetically determined through controlled intrathymic precursor T cell proliferation. *J Immunol* 181(11):7818–7824.
23. Hug A, et al. (2003) Thymic export function and T cell homeostasis in patients with relapsing remitting multiple sclerosis. *J Immunol* 171(1):432–437.
24. Bomberger C, et al. (1998) Lymphoid reconstitution after autologous PBSC transplantation with FACS-sorted CD34+ hematopoietic progenitors. *Blood* 91(7):2588–2600.
25. Jones JL, et al. (2009) IL-21 drives secondary autoimmunity in patients with multiple sclerosis, following therapeutic lymphocyte depletion with alemtuzumab (Campath-1H). *J Clin Invest* 119(7):2052–2061.
26. Kilpatrick RD, et al. (2008) Homeostasis of the naive CD4+ T cell compartment during aging. *J Immunol* 180(3):1499–1507.
27. den Braber I, et al. (2012) Maintenance of peripheral naive T cells is sustained by thymus output in mice but not humans. *Immunity* 36(2):288–297.
28. Stockinger H, et al. (1992) Phenotype of human T cells expressing CD31, a molecule of the immunoglobulin supergene family. *Immunology* 75(1):53–58.
29. Azevedo RI, et al. (2009) IL-7 sustains CD31 expression in human naive CD4+ T cells and preferentially expands the CD31+ subset in a PI3K-dependent manner. *Blood* 113(13):2999–3007.
30. Hazenberg MD, et al. (2000) Increased cell division but not thymic dysfunction rapidly affects the T-cell receptor excision circle content of the naive T cell population in HIV-1 infection. *Nat Med* 6(9):1036–1042.
31. Hu Y, et al. (2009) Investigation of the mechanism of action of alemtuzumab in a human CD52 transgenic mouse model. *Immunology* 128(2):260–270.
32. Moreau T, et al. (1996) Transient increase in symptoms associated with cytokine release in patients with multiple sclerosis. *Brain* 119(Pt 1):225–237.
33. Guimond M, et al. (2009) Interleukin 7 signaling in dendritic cells regulates the homeostatic proliferation and niche size of CD4+ T cells. *Nat Immunol* 10(2):149–157.
34. Fortner KA, Budd RC (2005) The death receptor Fas (CD95/APO-1) mediates the deletion of T lymphocytes undergoing homeostatic proliferation. *J Immunol* 175(7):4374–4382.
35. Workman CJ, Vignali DA (2005) Negative regulation of T cell homeostasis by lymphocyte activation gene-3 (CD223). *J Immunol* 174(2):688–695.
36. Strioga M, Pasukoniene V, Characiejus D (2011) CD8+ CD28- and CD8+ CD57+ T cells and their role in health and disease. *Immunology* 134(1):17–32.
37. Sun Z, et al. (2008) Association of Graves' disease and prevalence of circulating IFN-gamma-producing CD28(-) T cells. *J Clin Immunol* 28(5):464–472.
38. Dai H, et al. (2010) Cutting edge: Programmed death-1 defines CD8+CD122+ T cells as regulatory versus memory T cells. *J Immunol* 185(2):803–807.
39. Deaglio S, et al. (2007) Adenosine generation catalyzed by CD39 and CD73 expressed on regulatory T cells mediates immune suppression. *J Exp Med* 204(6):1257–1265.
40. Moxham VF, et al. (2008) Homeostatic proliferation of lymphocytes results in augmented memory-like function and accelerated allograft rejection. *J Immunol* 180(6):3910–3918.
41. Broadley SA, Deans J, Sawcer SJ, Clayton D, Compston DA (2000) Autoimmune disease in first-degree relatives of patients with multiple sclerosis. A UK survey. *Brain* 123(Pt 6):1102–1111.
42. Heinzlef O, et al. (2000) Autoimmune diseases in families of French patients with multiple sclerosis. *Acta Neurol Scand* 101(1):36–40.
43. Kappos L, et al. (2011) Ocrelizumab in relapsing-remitting multiple sclerosis: A phase 2, randomised, placebo-controlled, multicentre trial. *Lancet* 378(9805):1779–1787.
44. Habek M, et al. (2012) Thyroid autoimmunity in comparison of alemtuzumab and Rebif efficacy in multiple sclerosis studies I and II. *J Neurol* 259(Suppl 1):S1–S236.
45. Kirk AD, et al. (2003) Results from a human renal allograft tolerance trial evaluating the humanized CD52-specific monoclonal antibody alemtuzumab (CAMPATH-1H). *Transplantation* 76(1):120–129.
46. Knechtle SJ, et al. (2003) Campath-1H induction plus rapamycin monotherapy for renal transplantation: Results of a pilot study. *Am J Transplant* 3(6):722–730.
47. Wada T, Schurman SH, Garabedian EK, Yachie A, Candotti F (2005) Analysis of T-cell repertoire diversity in Wiskott-Aldrich syndrome. *Blood* 106(12):3895–3897.
48. Robins HS, et al. (2009) Comprehensive assessment of T-cell receptor beta-chain diversity in alphabeta T cells. *Blood* 114(19):4099–4107.